50 Gb/s On-Off-Keying over Duty-Cycle Division Multiplexing System with 10 GHz Clock

Ghafour Amouzad Mahdiraji, Amin Malekmohammadi, Ahmad Fauzi Abas, Safuraa Mohd Basir, Makhfudzah Mokhtar

Photonics and Fiber Optics Systems Laboratory, Centre of Excellence for Wireless and Photonics Networks, Engineering and Technology Complex, University Putra Malaysia, 43400 Serdang, Selangor, Malaysia

and

Mohamad Khazani Abdullah

Significant Technologies Sdn. Bhd. 43400 Serdang, Selangor, Malaysia

ABSTRACT

The performance of 5 × 10 Gb/s on-off-keying (OOK) modulation format over DCDM system is reported. The aggregate bit rate of 50 Gb/s is achieved with only 120 GHz spectral width. The clock and data recovery is realized at 10 GHz clock rate, which is very economic and efficient. The worst receiver sensitivity of –16.3 dBm, optical signal-to-noise ratio (OSNR) of 36 dB and chromatic dispersion tolerance of ±32 ps/nm are achieved. For the best channel, the receiver sensitivity, OSNR and chromatic dispersion tolerance are –26.5 dBm, 26.2 dB and ±69 ps/nm respectively.

Keywords: Optical Communications, Multiplexing, Duty-Cycle, On-Off-Keying, Clock Recovery.

1. INTRODUCTION

Optical communication forms the backbone of modern telecommunication and internet networks around the world. Improving transmission capacity of wavelength division multiplexing (WDM) is very important with a limited bandwidth [1]. In WDM systems, a wavelength can only carry one data channel. Time division multiplexing (TDM) is the most commonly used technique for multiplexing high number of lower bit rate channels to form a higher bit rate. For example, a 50 Gb/s data stream can be achieved by multiplexing five 10 Gb/s data using electrical TDM (ETDM) [2-7]. Synchronization for clock and data recovery is very important at such high speed aggregate bit rate [8-13]. Return-to-zero (RZ) line coding format facilitates system synchronization at the expense of higher spectral width. At 50 Gb/s, RZ-TDM has 200 GHz null-to-null spectral width and required transceiver operates at 50 GHz.

Recently, various advanced multiplexing techniques and modulation formats are developed to increase the transmission capacity of WDM systems with transceiver operates at signal baud/symbol rate [14-26]. Differential quadrature phase-shift-keying (DQPSK) [21-23, 25] and polarization division multiplexing (PDM) [14, 15, 24] are example of such techniques, which doubles transmission capacity of WDM channel. Combining DQPSK with PDM quadruples WDM network capacity [16-20, 26], however such systems is very complex and costly.

Duty-cycle division multiplexing (DCDM) for optical communication system was introduced in [27, 28], which implements direct detection and able to support the transmission of multi-channel per WDM channel. This technique is implemented based on RZ duty cycle, in which different channels are assigned with different RZ duty cycle values. This technique provides self symbol synchronization due to a rising edge transition at the beginning of each symbol in the multiplexed signal, which allows the receiver to operate at symbol rate for clock and data recovery. Using this technique, relatively small spectral width is resulted. Performance of three 10 Gb/s amplitude-shift-keying (ASK) channels over DCDM was reported in [29]. In this paper, for the first time, we analyze the performance of 5 channels referring to back-to-back receiver sensitivity, optical signal-to-noise ratio (OSNR), chromatic dispersion tolerance and spectral width. We have shown that, 5 × 10 Gb/s DCDM data can be recovered by using 10 GHz clock with 120 GHz null-to-null spectral width.

2. SIMULATION SETUP

Fig. 1 (a) shows the simulation setup of DCDM system for multiplexed 5 channels. User1 (U1) to User5 (U5), each with 10 Gb/s pulse at PRBS 2^{10}–1, are curved using 5 RZ pulse generators, which generate different duty cycles (DCs). The DCs are distributed uniformly between different channels, which the i^{th} RZ pulse generator has a DC of T_i calculated from the following equation.

$$T_i = \frac{i \times T_s}{n+1} \qquad (1)$$

where T_s represents the multiplexed symbol duration and n is the number of multiplexing users.

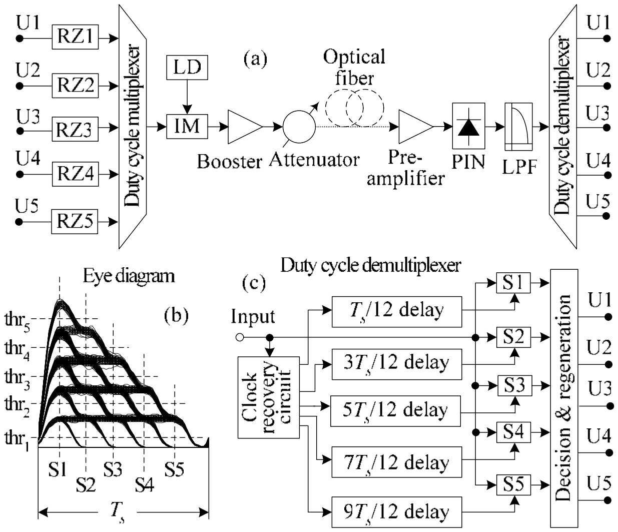

Fig. 1. (a) DCDM simulation setup for multiplexing 5 users, (b) eye diagram and (c) demultiplexer.

These RZ signals each with different DCs were synchronously multiplexed using an electrical adder. The output of the multiplexer was then modulated with a laser diode (LD) signal, which operated at 1550 nm wavelength using an intensity modulator (IM) (here amplitude modulator (AM) with infinity extinction ratio is used). Output of the modulator is a step shape signal or multilevel signal whereby the amplitude of each level is uniformly distributed. Fig. 1 (b) shows a back-to-back eye diagram for the multiplexed 5 channels measured at BER of 10^{-9}. Fig. 2 illustrates example of the working principle of the system in more detail for 5 channels. Fig. 2 (b), (c), (d), (e) and (f) show the output signals of the RZ signal generator number 1, 2, 3, 4 and 5 with 16.6%, 33.3%, 50%, 66.6% and 83.3% DC respectively. The generated signals are based on the bits represented in Fig. 2 (a). Fig. 2 (g) shows the 32 unique multiplexed patent signals for the 5 channels.

At the receiver side, the optical signal is detected by a PIN photodiode and passed through a low-pass filter (LPF) followed by a demultiplexer. The Gaussian electrical LPF is used in order to minimize additional dispersion and noises with a cut-off frequency of 45 GHz. In the demultiplexer (Fig. 1 (c)), the clock recovery circuit has an external clock, which oscillates at the frequency equal with the symbol rate (10 GHz). This 10 GHz clock can be recovered from the received signal spectra by detecting the 10 GHz impulse transition using phase lock loop (PLL). This impulse transition is shown in Fig. 3. The oscillator is resynchronized to each rising edge of the input signal as there is a rising edge transition per symbol, which appears at the beginning of the symbol. The 5 sampling circuits are synchronized with the recovered clock. By putting an appropriate delay lines [30] for each of the sampler as shown in Fig. 1 (b), the 1st, 2nd, …, and 5th sampler (S_1, S_2, …, and S_5) take samples at $T_s/12$, $3T_s/12$, …, and $9T_s/12$ s per symbol respectively. The frequency of all samplers is equal to the symbol rate. Outputs of the samplers are fed into the decision and regeneration unit. In this unit, the sampled values are compared against 5 threshold values, thr_1, thr_2, …, and thr_5. Decision is made for U1 based on the information taken from the two consecutive sampling points, S_1 and S_2. If amplitudes of those two adjacent sampling points are equal, bit 0 is recovered (for example, cases 1, 3, 5, 7, 9, 11, 13, 15, 17, 19, 21, 23, 25, 27, 29 and 31 from Fig. 2 (g)). On the other hand, when the amplitude at S_1 is one level greater than S_2, bit 1 is regenerated (cases 2, 4, 6, 8, 10, 12, 14, 16, 18, 20, 22, 24, 26, 28, 30 and 32). The same method is used for U2, which utilizes information extracted from S_2 and S_3. Only the last channel, U5, is recovered by comparing amplitude of only S_5 against thr_1. Table 1 shows example of the rules designed for U1 and U2 in 5-channel system in all cases given in Fig. 2 (g). Bit error rate (BER) in this paper is calculated based on the probability of error method.

(a)

Cases	1	2	3	4	5	6	7	8	9	10	11	12	13	14	15	16	17	18	19	20	21	22	23	24	25	26	27	28	29	30	31	32
U1	0	1	0	1	0	1	0	1	0	1	0	1	0	1	0	1	0	1	0	1	0	1	0	1	0	1	0	1	0	1	0	1
U2	0	0	1	1	0	0	1	1	0	0	1	1	0	0	1	1	0	0	1	1	0	0	1	1	0	0	1	1	0	0	1	1
U3	0	0	0	0	1	1	1	1	0	0	0	0	1	1	1	1	0	0	0	0	1	1	1	1	0	0	0	0	1	1	1	1
U4	0	0	0	0	0	0	0	0	1	1	1	1	1	1	1	1	0	0	0	0	0	0	0	0	1	1	1	1	1	1	1	1
U5	0	0	0	0	0	0	0	0	0	0	0	0	0	0	0	0	1	1	1	1	1	1	1	1	1	1	1	1	1	1	1	1

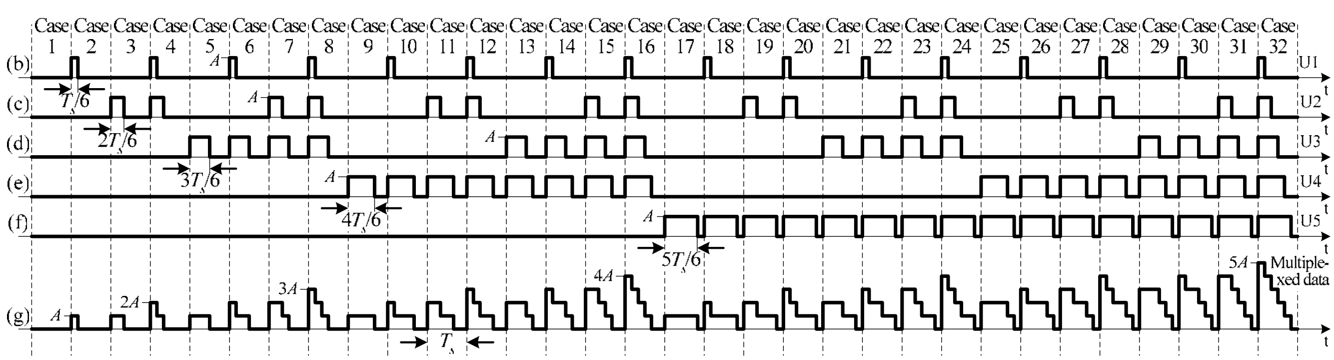

Fig. 2. (a) 32 possible combinations of bits for 5-user, (b), (c), (d), (e) and (f) signals for U1, U2, U3, U4 and U5 respectively, and (g) multiplexed signals.

Table 1. Data recovery rules of 5-user DCDM system for U1 and U2 based on the signals represented in Fig. 2 (g).

Rules for U1							Cases
1	if	$(S_1 < thr_1)$	&	$(S_2 < thr_1)$,	then	U1=0	1
2	if	$(thr_1 \le S_1 < thr_2)$	&	$(thr_1 \le S_2 < thr_2)$,	then	U1=0	3,5,9,17
3	if	$(thr_2 \le S_1 < thr_3)$	&	$(thr_2 \le S_2 < thr_3)$,	then	U1=0	7,11,13,19,21,25
4	if	$(thr_3 \le S_1 < thr_4)$	&	$(thr_3 \le S_2 < thr_4)$,	then	U1=0	15,23,27,29
5	if	$(thr_4 \le S_1 < thr_5)$	&	$(thr_4 \le S_2 < thr_5)$,	then	U1=0	31
6	if	$(thr_1 \le S_1 < thr_2)$	&	$(S_2 < thr_1)$,	then	U1=1	2
7	if	$(thr_2 \le S_1 < thr_3)$	&	$(thr_1 \le S_2 < thr_2)$,	then	U1=1	4,6,10,18
8	if	$(thr_3 \le S_1 < thr_4)$	&	$(thr_2 \le S_2 < thr_3)$,	then	U1=1	8,12,14,20,22,26
9	if	$(thr_4 \le S_1 < thr_5)$	&	$(thr_3 \le S_2 < thr_4)$,	then	U1=1	16,24,28,30
10	if	$(S_1 \ge thr_5)$	&	$(S_2 \ge thr_4)$,	then	U1=1	32
Rules for U2							Cases
1	if	$(S_2 < thr_1)$	&	$(S_3 < thr_1)$,	then	U2=0	1,2
2	if	$(thr_1 \le S_2 < thr_2)$	&	$(thr_1 \le S_3 < thr_2)$	then	U2=0	5,6,9,10,17,18
3	if	$(thr_2 \le S_2 < thr_3)$	&	$(thr_2 \le S_3 < thr_3)$	then	U2=0	13,14,21,22,25,26
4	if	$(thr_3 \le S_2 < thr_4)$	&	$(thr_3 \le S_3 < thr_4)$	then	U2=0	29,30
5	if	$(thr_1 \le S_2 < thr_2)$	&	$(S_3 < thr_1)$,	then	U2=1	3,4
6	if	$(thr_2 \le S_2 < thr_3)$	&	$(thr_1 \le S_3 < thr_2)$,	then	U2=1	7,8,11,12,19,20
7	if	$(thr_3 \le S_2 < thr_4)$	&	$(thr_2 \le S_3 < thr_3)$,	then	U2=1	15,16,23,24,27,28
8	if	$(S_2 \ge thr_4)$	&	$(S_3 \ge thr_3)$,	then	U2=1	31,32

3. RESULTS AND DISCUSSIONS

DCDM provides a rising edge transition at the beginning of each multiplexed symbol, except for the case that bit 0 is transmitted by all channels (case 1 in Fig. 2), which has very low possibility to occur, particularly as the number of channels increases. The rising edge transition per symbol is highlighted in Fig. 2 (e), which shows an example of the multiplexed signals for 3-channel system. By detecting this rising edges, the beginning of each multiplexed symbol will be determined. Therefore, unlike TDM systems, this system does not require extra information and processing for symbol synchronization.

As explained in the previous section, using a delay line and a sampling circuit per channel, the received bit stream can be recovered at symbol rate. This leads the system towards the utilization of lower end clock recovery circuits with lower speed electronic components. With reference to conventional TDM at the same aggregate bit rate, our solution offers lower cost.

In addition to that, DCDM offers great saving in the spectral width. As shown in Fig. 3, using DCDM technique, the maximum null-to-null spectral width of 50 Gb/s RZ-TDM (200 GHz) is reduced to 120 GHz. The spectral width of RZ-TDM reduces by 40%. This saving in the spectral width increases as the number of channels increases. This is because DCDM signals require a null-to-null spectral width of $2 \times [(n + 1) / n] \times R_{aggrigated}$, whereas RZ-TDM requires $4 \times R_{aggrigated}$ where, $R_{aggrigated}$ is the system aggregated/total bit rate. Based on this feature, better spectral efficiency is expected.

Fig. 4 and 5 show the back-to-back pre-amplified receiver sensitivity and OSNR of 5 × 10 Gb/s DCDM technique. A receiver sensitivity of around –16.3 dBm is obtained for the worst user (U1), for the system to achieve BER of 10^{-9}. Meanwhile, the best user (U5) has receiver sensitivity of around –26.5 dBm at the same BER. In terms of OSNR, at the same BER, an OSNR of 36 dB and 26.2 dB is required for the worst and the best user in the system respectively.

The different performance for different users in DCDM technique is due to the number of eyes participating in the BER calculation for the different users from one side; and different performance for different eyes from the other side. Table 2 shows the Q-factor, eye amplitude/optical modulation amplitude (OMA) and eye closer for those 15 eyes shown in Fig. 6. In this table, for each individual eye, the Q-factor (Q), eye amplitude (E_A)/OMA and eye closer (E_C) are calculated respectively as following [31-33],

$$Q = \frac{|\mu_1 - \mu_0|}{\sigma_1 + \sigma_0} \tag{2}$$

$$E_A = \mu_1 - \mu_0 \tag{3}$$

$$E_C = \min(V_1) - \max(V_0) \tag{4}$$

where μ_i and σ_i represent the mean and standard deviation of binary $i = 0, 1$, at sampling point respectively. $\min(V_1)$ is the minimum value of the amplitude for binary 1, and $\max(V_0)$ is the maximum value for the amplitude of binary 0. As explained in the previous section, BER of the 1st user is calculated based on the 1st and the 2nd slots (S_1 and S_2), which has the most number of eyes (eye number 1 to eye number 9 from Fig. 6). On the other hand, BER of the last user (U5) relates to only one eye, which appears at the last slot, S_5 (eye number 15 from Fig. 6).

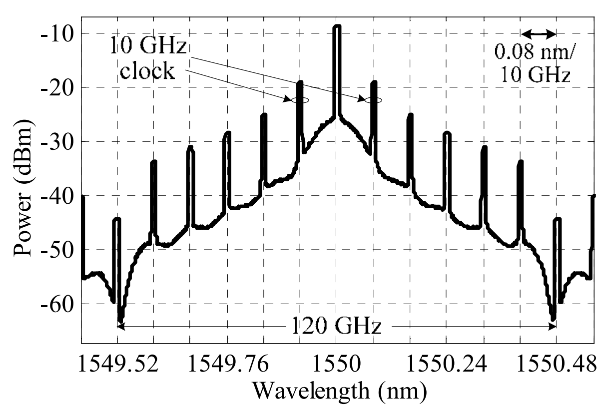

Fig. 3. Spectral width of 5 × 10 Gb/s DCDM multiplexed signals.

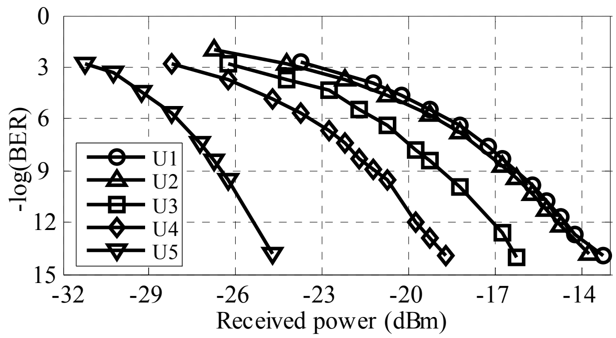

Fig. 4. Pre-amplified receiver sensitivity for 5 × 10 Gb/s DCDM system.

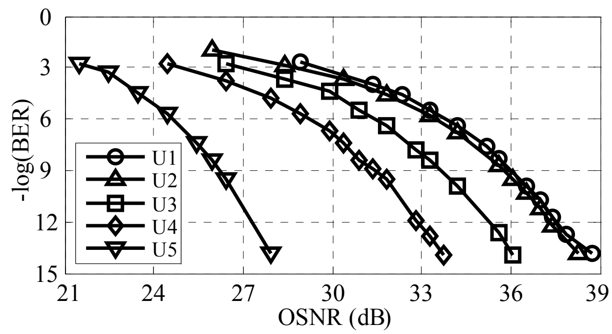

Fig. 5. OSNR for 5 × 10 Gb/s DCDM system.

Since different eyes show different quality, performance of different users are different. For example, as shown in Table 2 and Fig. 6, the Eye 1 has the least OMA and eye opening, which results in the least Q-factor and then the largest BER. Whereas, the Eye 15 has larger OMA and eye opening, thus better Q-factor and BER in comparison to the Eye 1. Therefore, it is clear that in the proposed system, U5 always has better performance than the other users. On the other hand, U1 has the worst performance amongst the multiplexed users.

Table 2. Q-factor, eye amplitude/OMA and eye closer for the eyes represented in Fig. 6

No. of Eye	Q-factor	Eye amplitude/ OMA (mW)	Eye closer (mW)
Eye 1	**5.90783**	**0.00354**	**0.00200**
Eye 2	6.33508	0.00350	0.00202
Eye 3	7.73202	0.00352	0.00214
Eye 4	9.79202	0.00351	0.00260
Eye 5	21.68518	0.00351	0.00312
Eye 6	6.24397	0.00353	0.00211
Eye 7	7.38278	0.00355	0.00191
Eye 8	9.96054	0.00356	0.00256
Eye 9	21.00377	0.00355	0.00317
Eye 10	7.70917	0.00354	0.00222
Eye 11	9.98918	0.00353	0.00240
Eye 12	22.28425	0.00353	0.00300
Eye 13	10.33203	0.00351	0.00261
Eye 14	20.41372	0.00353	0.00304
Eye 15	**22.10611**	**0.00347**	**0.00303**

Fig. 7 shows the effect of chromatic dispersion on 5 × 10 Gb/s DCDM signals. Based on the results, the worst user can tolerate chromatic dispersion of ±32 ps/nm and the best channels can support the dispersion of ±69 ps/nm at BER of 10^{-9}. The different performance between different users is due to the same reason that explained above for receiver sensitivity and OSNR.

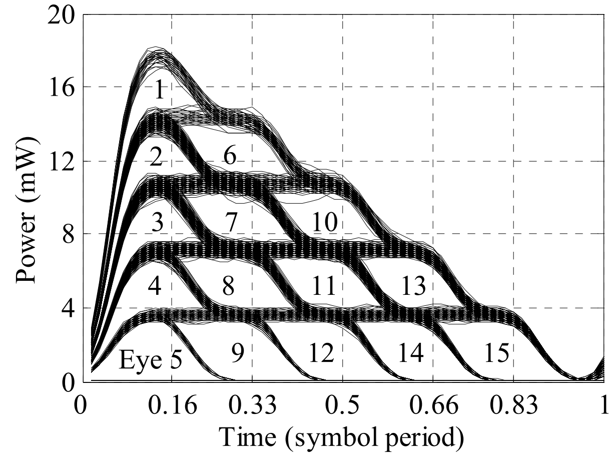

Fig. 6. Eye diagram of 5 × 10 Gb/s DCDM signal measured at received power of –16.25 dBm (around BER of 10^{-9}).

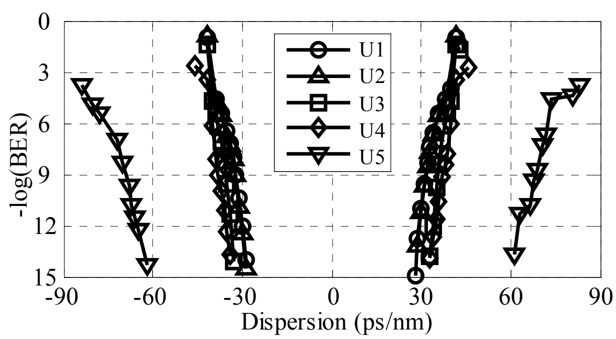

Fig. 7. Chromatic dispersion tolerance of 5 × 10 Gb/s DCDM signals.

4. CONCLUSION

DCDM technique with the capacity of 5 × 10 Gb/s is reported. Performance of DCDM was assessed in terms of back-to-back receiver sensitivity, OSNR, and chromatic dispersion tolerance. Due to the rising edge transition at the beginning of each multiplexed symbol, this technique allowed the 50 Gb/s data stream to be recovered using an external clock and 5 sampling circuits that all running at 10 GHz, which results in a lower speed of electronic component thus reducing cost. With 120 GHz spectral width this technique reduces 40% spectral width of RZ-TDM.

5. REFERENCES

[1] H. Jumpei, K. Kasai, M. Yoshida, and M. Nakazawa, "1 Gsymbol/s, 64 QAM coherent optical transmission over 150 km

with a spectral efficiency of 3 bit/s/Hz," in *Proceeding Optical Fiber Communication Conference/ National Fiber Optic Engineers Conference* (*OFC/NFOEC*), 2007, pp. 1-3.

[2] P. M. Krummrich, E. Gottwald, C.J. Weiske, A. Schopflin, I. Kotten, and B. Lankl, "40 Gbit/s ETDM for long haul WDM transmission," in *15th Annual Meeting of the IEEE Lasers and Electro-Optics Society* (*LEOS*), 2002, pp. 71-72.

[3] E. Lach, H. Bulow, M. Kaiser, G. Veith, and S. Bouchoule, "40 Gbit/s TDM field test over 111 km installed G.652 fiber," in *24th European Conference on Optical Communication* (*ECOC*), 1998, pp. 687-688.

[4] W.S. Lee, D. Garthe, G.A. Pettitt, and A.A. Hadjifotiou, "40-Gbit/s TDM transmission over 160 km (2 × 80 km) of standard nondispersion-shifted fiber," in *Proceeding Optical Fiber Communication Conference* (*OFC*), 1997, pp. 244-245.

[5] Y. Miyamoto, M. Yoneyama, T. Otsuji, K. Yonenaga, and N. Shimizu, "40-Gbit/s TDM transmission technologies based on ultra-high-speed ICs," *IEEE Journal of Solid-State Circuits,* vol. 34, pp. 1246-1253, 1999.

[6] L. Dong-Soo, L. Man Seop, W. Yang Jing, and A. Nirmalathas, "Electrically band-limited CSRZ signal with simple generation and large dispersion tolerance for 40-Gb/s WDM transmission systems," *IEEE Photonics Technology Letters,* vol. 15, pp. 987-989, 2003.

[7] M. Yoneyama, Y. Miyamoto, T. Otsuji, A.A. Hirano, H. A. Kikuchi, T.A. Ishibashi, and H.A. Miyazawa, "Fully electrical 40-Gbit/s TDM system prototype and its application to 160-Gbit/s WDM transmission," in *Proceeding Optical Fiber Communication Conference/ International Conference on Integrated Optics and Optical Fiber Communication* (*OFC/IOOC*), 1999, pp. 128-130.

[8] H. Tsuchida and M. Suzuki, "40-Gb/s optical clock recovery using an injection-locked optoelectronic oscillator," *IEEE Photonics Technology Letters,* vol. 17, pp. 211-213, 2005.

[9] H. Tsuchida, "160-gb/s optical clock recovery using a regeneratively mode-locked laser diode," *IEEE Photonics Technology Letters,* vol. 18, pp. 1687-1689, 2006.

[10] L. Ju Han, S. Ohara, T. Nagashima, T. Hasegawa, N. Sugimoto, K. Igarashi, K. Katoh, and K. Kikuchi, "Clock recovery and demultiplexing of high-speed OTDM signal through combined use of bismuth oxide nonlinear fiber and erbium-doped bismuth oxide fiber," *IEEE Photonics Technology Letters,* vol. 17, pp. 2658-2660, 2005.

[11] E. Tangdiongga, J.P. Turkiewicz, G.D. Khoe, and H.d. Waardt, "Clock recovery by a fiber ring laser employing a linear optical amplifier," *IEEE Photonics Technology Letters,* vol. 16, pp. 611-613, 2004.

[12] S. Yufei and G. Ning, "Dual-stage clock recovery for TDM in packet networks," in *IEEE International Symposium on Communications and Information Technology,* 2005, pp. 1051-1053.

[13] B. Razavi, "Challenges in the design high-speed clock and data recovery circuits," in *IEEE Communications Magazine*, vol. 40, Aug 2002, pp. 94-101.

[14] S. Bigo, Y. Frignac, G. Charlet, W. Idler, S. Borne, H. Gross, R. Dischler, W. Poehlmann, P. Tran, C. Simonneau, D. Bayart, G. Veith, A. Jourdan, and J.P. Hamaide, "10.2 Tbit/s (256 × 42.7 Gbit/s PDM/WDM) transmission over 100 km TeraLight™ fiber with 1.28 bit/s/Hz spectral efficiency," in *Proceeding Optical Fiber Communication Conference* (*OFC*), 2001, PD25-1-PD25-3.

[15] L.S. Yan, B. Zhang, A. Belisle, A.E. Willner, and X.S. Yao, "Automatic all-optical detection in polarization-division-multiplexing system using power unbalanced transmission," in *Conference on Lasers and Electro-Optics,* 2007, pp. 1-2.

[16] G. Charlet, J. Renaudier, H. Mardoyan, P. Tran, O.B. Pardo, F. Verluise, M. Achouche, A. Boutin, F. Blache, J.-Y. Dupuy, and S. Bigo, "Transmission of 16.4 Tbit/s capacity over 2,550 km using PDM QPSK modulation format and coherent receiver," in *Proceeding OFC/NFOEC*, 2008, Paper PDP3.

[17] O.B. Pardo, J. Renaudier, H. Mardoyan, P. Tran, G. Charlet, and S. Bigo, "Investigation of design options for overlaying 40 Gb/s coherent PDM-QPSK channels over a 10 Gb/s system infrastructure," in *Proceeding OFC/NFOEC*, 2008, pp. 1-3.

[18] A.F. Abas, A. Hidayat, D. Sandel, B. Milivojevic, and R. Noe, "100 km fiber span in 292 km, 2.38 Tb/s (16 × 160 Gb/s) WDM DQPSK polarization division multiplex transmission experiment without Raman amplification," *Optical Fiber Technology,* vol. 13, pp. 46-50, 2007.

[19] A.H. Gnauck, G. Charlet, P. Tran, P. Winzer, C. Doerr, J. Centanni, E. Burrows, T. Kawanishi, T. Sakamoto, and K. Higuma, "25.6-Tb/s C+L-band transmission of polarization-multiplexed RZ-DQPSK signals," in *Proceeding OFC/NFOEC*, 2007, Paper PDP19.

[20] A.H. Gnauck, G. Charlet, P. Tran, P.J. Winzer, C.R. Doerr, J.C. Centanni, E.C. Burrows, T. Kawanishi, T. Sakamoto, and K. Higuma, "25.6-Tb/s WDM transmission of polarization-multiplexed RZ-DQPSK signals," *Journal of Lightwave Technology,* vol. 26, pp. 79-84, 2008.

[21] A.H. Gnauck, P.J. Winzer, C. Dorrer, and S. Chandrasekhar, "Linear and nonlinear performance of 42.7-Gb/s single-polarization RZ-DQPSK format," *IEEE Photonics Technology Letters,* vol. 18, pp. 883-885, 2006.

[22] T. Kawanishi, T. Sakamoto, T. Miyazaki, M. Izutsu, K. Higuma, and J. Ichikawa, "80 Gb/s DQPSK modulator," in *Proceeding OFC/NFOEC*, 2007, pp. 1-3.

[23] I. Lyubomirsky, C. Cheng-Chung, and W. Yi-Hsiang, "Optical DQPSK receiver with enhanced dispersion tolerance," *IEEE Photonics Technology Letters,* vol. 20, pp. 511-513, 2008.

[24] P. Martelli, P. Boffi, M. Ferrario, L. Marazzi, P. Parolari, S. M. Pietralunga, A. Righetti, R. Siano, M. Torregiani, and M. Martinelli, "Endless polarization stabilizer for high bit-rate polarization-division multiplexed optical systems," in *Proceeding OFC/NFOEC*, 2008, pp. 1-3.

[25] D. van den Borne, S.L. Jansen, E. Gottwald, E.D. Schmidt, G.D. Khoe, and H. de Waardt, "DQPSK modulation for robust optical transmission," in *Proceeding OFC/NFOEC*, 2008, pp. 1-3.

[26] C. Wree, N. Hecker-Denschlag, E. Gottwald, P. Krummrich, J. Leibrich, E.D. Schmidt, B. Lankl, and W. Rosenkranz, "High spectral efficiency 1.6-b/s/Hz transmission (8 × 40 Gb/s with a 25-GHz grid) over 200-km SSMF using RZ-DQPSK and polarization multiplexing," *IEEE Photonics Technology Letters,* vol. 15, pp. 1303-1305, 2003.

[27] M.K. Abdullah, M.F. Abdalla, A.F. Abas, and G.A. Mahdiraji, "Duty-cycle division multiplexing (DCDM): A novel and economical optical multiplexing and electrical demultiplexing technique for high speed fiber optics networks," in *International Conference on Wireless and Optical Communications Networks* (*WOCN*), 2007, pp. 1-4.

[28] G.A. Mahdiraji, M.K. Abdullah, A.F. Abas, M. Mokhtar, and A.M. Mohammadi, "Analysis of the transmission performance of optical signals based on duty cycle division multiplexing (DCDM)," in *6th National Conference on Telecommunication Technologies and 2nd Malaysia Conference on Photonics* (*NCTT-MCP*), Malaysia, 2008, ID93.

[29] G.A. Mahdiraji, A.M. Mohammadi, A.F. Abas, M.K. Abdullah, and M. Mokhtar, "A novel economical duty cycle division multiplexing with electrical multiplexer and demultiplexer for optical communication systems," in *IEEE International Conference on Electronic Design* (*ICED*), 2008, pp. 1-5.

[30] L. Chen, Q. Zhu, and S. Xu, "Delay lines based on left-handed transmission line structure," in *IEEE International Symposium on Antennas and Propagation Society*, 2006, pp. 1189-1192.

[31] S. Ohteru and N. Takachio, "Optical signal quality monitor using direct Q-factor measurement," *IEEE Photonics Technology Letters,* vol. 11, pp. 1307-1309, 1999.

[32] N.S. Bergano, F.W. Kerfoot, and C.R. Davidson, "Margin measurements in optical amplifier systems," *IEEE Photonics Technology Letters,* vol. 5, pp. 304-306, 1993.

[33] C.J. Anderson and J.A. Lyle, "Technique for evaluating system performance using Q in numerical simulations exhibiting intersymbol interference," *Electronics Letters,* vol. 30, pp. 71-72, 1994.